

## Drying characteristics of a Japanese dry-cured ham model: Effect of temperature and humidity

<sup>1,2\*</sup>Kato, K., <sup>1</sup>Tanji, H. and <sup>2</sup>Ichikawa, S.

<sup>1</sup>Prima Meat Packers Ltd., Nakamukaihara 635, Tsuchiura, Ibaraki 300-0841, Japan

<sup>2</sup>Faculty of Life and Environmental Sciences, University of Tsukuba, Tennodai 1-1-1, Tsukuba, Ibaraki 305-8572, Japan

### Article history

Received:  
30 April 2021

Received in revised form:  
21 March 2022

Accepted:  
16 June 2022

### Keywords

dry-cured ham,  
moisture diffusivity,  
relative humidity,  
activation energy,  
magnetic resonance imaging  
(MRI)

### Abstract

The drying characteristics of a Japanese dry-cured ham model containing uniformly distributed brine were investigated. A higher effective moisture diffusivity was obtained at a lower relative humidity (RH) level. The activation energy of effective moisture diffusivity at 40 and 70% RH increased with decreasing moisture content, and was almost constant in the late stage of drying. Therefore, the moisture likely diffused without a large difference in the moisture distribution in the sample. In contrast, under low (10%) RH, the activation energy drastically increased with decreasing moisture content in the initial stage of drying. From the results of magnetic resonance imaging, the moisture content on the surface was drastically decreased; the surface was dried and hardened temporarily (*i.e.*, case hardening) by the fast transfer of moisture. In the middle to late stages of drying, the activation energy gradually decreased to the similar values as at 40 and 70% RH in the late stage of drying. From the results of magnetic resonance imaging analysis after drying, the moisture distribution near the surface no longer exhibited a sharp difference in moisture concentration. The partly dried state of the surface could be alleviated by the transfer of moisture from the inside of the sample. Comparing the energy consumption for drying up to 175% dry basis, the drying condition of 35°C and 40% RH was the most efficient.

### DOI

<https://doi.org/10.47836/ifrj.29.6.19>

© All Rights Reserved

### Introduction

Drying is important in the food industry. Drying results in microbial control and flavour development, but over- and under-drying must be avoided to preserve hygiene and quality. Therefore, to maintain hygiene and quality of dried food, it is necessary to optimise drying. A moisture transfer model based on moisture diffusion is commonly used for optimising the drying conditions, but this model depends on the type and form of the food (Panagiotou *et al.*, 2004). Moisture transfer occurs in food during drying. Moisture transfer by diffusion is caused by a moisture concentration gradient as the driving force. Generally, ventilation drying can be roughly divided into two drying periods: a constant-rate period in which the drying rate is constant, and a falling-rate period in which the drying rate gradually decreases as drying progresses. For drying food, the falling rate period is almost always used. During the falling-rate period, the rate of transfer of the internal moisture of the dry material to the surface is the rate-determining

step. In this case, the moisture transfer of the food is governed by the effective moisture diffusivity ( $D_e$ ). Therefore, the drying behaviour of food has been studied in relation to the  $D_e$  and the activation energy.

Typical meat products that employ drying are dry-cured meats and salami sausage (Petrova *et al.*, 2015). The drying of meat is generally considered to be a diffusive process. In accordance with Fick's diffusion law, the moisture gradient and the  $D_e$  of the meat affect moisture diffusion. Moisture diffusion is important in meat-drying (Hallström, 1990). Studies on the  $D_e$  of raw meat have been reported using different types of meat and processed meat products as listed in Table 1. In these studies, the dependency of  $D_e$  on the temperature is generally described by the Arrhenius equation, as is the case for most food products (Okos *et al.*, 1992).

A common method of salting dry-cured ham, such as prosciutto, is to apply dry salt to the surface. However, some Japanese dry-cured ham is produced using raw meat pre-treated with a brine injector (Tanaka *et al.*, 2000). In this brine-injection method,

\*Corresponding author.

Email: Keiichi.Katou@primaham.co.jp

**Table 1.** Effective moisture diffusivity of meat and processed meat products.

Material	Temperature (°C)	Effective moisture diffusivity $D_e$ [ $m^2/s$ ]	Reference
Beef meat	40 - 60	$2.32 - 5.59 \times 10^{-10}$	Mewa <i>et al.</i> (2018)
Chicken breast meat	60	$9.96 \times 10^{-10}$	Ismail (2017)
Turkey breast meat	60	$2.03 \times 10^{-10}$	Elmas <i>et al.</i> (2020)
Pork ham muscle	5	$0.31 - 0.49 \times 10^{-10}$	Gou <i>et al.</i> (2002)
Dry-cured ham	19	$0.239 - 0.779 \times 10^{-10}$	Gou <i>et al.</i> (2004)
Japanese dry-cured ham model	18	$2.10 - 13.9 \times 10^{-10}$	The present work
	27	$3.16 - 16.5 \times 10^{-10}$	
	35	$4.11 - 17.9 \times 10^{-10}$	

a needleless injector is used to inject brine into raw meat at high pressure. As a result, the raw meat contains salt that is uniformly distributed to the centre, hence the salting processing time can be greatly shortened. Furthermore, the moisture content of meat pre-treated by this method is less than that determined by the dry salting method. For example, the initial moisture content of surface-salted ham has been measured as 278.8% dry basis (d.b.) (Gou *et al.*, 2003), whereas that of brine-injected ham was approximately 245% d.b. as a model sample in the present work. The dry-cured ham widely distributed in Japan has a high moisture content (approximately 175% d.b., when compared with 100% d.b. in typical European dry-cured ham) and soft texture, unlike the dry-cured ham (prosciutto) that is typical in Europe. Therefore, Japanese dry-cured ham has a low initial moisture content, and a high moisture content at the end of drying, hence the time required for drying can be shortened.

The initial moisture content and the salt distribution affect the drying behaviour of raw ham (Gou *et al.*, 2003; Petrova *et al.*, 2015). A study of the moisture diffusion in dry-cured ham pre-treated by the dry-salting method has been reported (Gou *et al.*, 2002; 2003), but the drying behaviour of brine-injected ham that is used to produce Japanese dry-cured ham has not been studied. The aim of the present work was therefore to determine the  $D_e$  of a Japanese dry-cured ham model containing uniformly distributed brine under different drying conditions, and to analyse the moisture transfer in relation to the changes in the activation energy and the moisture distribution inside a Japanese dry-cured ham model as determined by magnetic resonance imaging (MRI). Furthermore, the energy consumption in the different drying conditions was evaluated in the context of practical applications.

## Materials and methods

### Sample preparation

A model of Japanese dry-cured ham was prepared by mixing minced pork meat and brine. Frozen pork was thawed in a refrigerator (4°C), and minced with a chopper. The brine was prepared by dissolving 18% w/w sodium chloride and 0.04% w/w sodium nitrite in water. The brine (30 parts by weight) was added to the raw minced meat (100 parts by weight) and mixed with an electric mixer for 5 min. The weight of the sample was approximately 220 g, and had an initial moisture content ( $W_D$ ) of 245% d.b. After overnight storage in a refrigerator (4°C), the mixture was placed into a water-vapour-permeable casing (50 mm in diameter and 100 mm in length) by using a filling machine, and this was used as a cylindrical sample for the drying experiments.

### Drying experiments

A constant temperature and humidity chamber (PDR-3J, ESPEC Corp., Japan) was used for the drying experiments. The inner dimensions of the chamber were 600 × 800 × 850 mm (W × D × H). The three samples were suspended in the drying chamber. The weight changes of each sample were measured with microload cells (LVS-A, Kyowa Denki KK, Japan), and directly recorded with a personal computer during the drying experiments (Figure 1).

The drying experiments were performed at temperatures ( $T_D$ ) of 18, 27, and 35°C, and relative humidity (RH) values of 10, 40, and 70%. The wind velocity close to the sample was approximately 1.0 m/s. The weights during the drying experiments were recorded at 5-min intervals. The dry basis moisture content ( $W$ ) was calculated by the weight ratio of moisture to the anhydrous material (dry solid) of the

sample. The weight of the dry solid sample was measured by an oven-drying method.

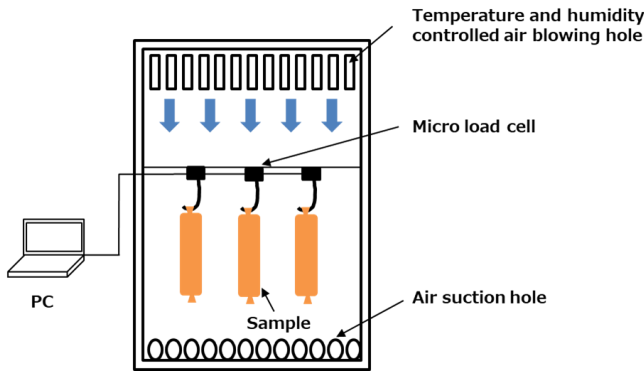


**Figure 1.** Schematic of the drying experiments of the Japanese dry-cured ham model with a constant temperature and humidity chamber.

#### Effective moisture diffusivity

The  $D_e$  during the drying experiment was calculated by the approximate formula of Carslaw and Jaeger (1959) and Konishi and Kobayashi (1999) as shown in Eq. 1:

$$W_R = \frac{W - W_e}{W_D - W_e} \quad (\text{Eq. 1})$$

where,  $W_R$  (-): moisture ratio;  $W$  (% d.b.): moisture content;  $W_D$  (% d.b.): initial moisture content of sample; and  $W_e$  (% d.b.): equilibrium moisture content (at  $t = \infty$ ).

The values of  $D_e$  were calculated using Eq. 2:

$$W_R = \left(\frac{8}{\pi^2}\right)^3 \exp\left(-D_e t \left(\frac{\pi^2}{4}\right) \left(\frac{2}{(kr)^2} + \frac{4}{h^2}\right)\right) \quad (\text{Eq. 2})$$

where,  $D_e$  ( $\text{m}^2/\text{s}$ ): effective moisture diffusivity;  $t$  (h): time;  $r$  (m): cylinder radius;  $h$  (m): cylinder height; and  $k$  (-): coefficient for surface area correction (0.816 in the test sample).

#### Activation energy

The correlation between the diffusion coefficient and drying temperature is generally expressed by an Arrhenius-type equation. The activation energy ( $E_a$ ) was calculated using Eq. 3 by the  $D_e$  value at the drying temperatures of 18, 27, and 35°C:

$$D_e = D_e^0 \exp\left(-\frac{E_a}{RT}\right) \quad (\text{Eq. 3})$$

where,  $E_a$  (J/mol): activation energy;  $R$  (J/(K mol)): gas constant;  $T$  (K): temperature; and  $D_e^0$  ( $\text{m}^2/\text{s}$ ): constant for diffusion coefficient at infinite temperature.

#### MRI analysis

$^1\text{H}$  MRI was performed with a nuclear magnetic resonance (NMR) spectrometer (DRX 300WB, Bruker, Germany) in accordance with a previous study (Sekiyama *et al.*, 2012). A dry-cured ham model was cut into pieces measuring 20 mm in length. The sample was placed in an NMR tube (25 mm, inside diameter) for MRI measurement. A multi-slice multi-echo pulse sequence (MSME in Bruker library) was used to measure the spin-spin relaxation time (in milliseconds),  $T_2$ , of protons in each voxel of the sample. The analysis settings were as follows: repetition time, 5 s; echo time, 5 ms; number of echoes with a constant interval of 4 ms, 32; field of view (FOV), 20 × 20 mm; imaging matrix size, 128 × 128; and slice thickness, 1 mm. The spatial resolution was 156 × 156  $\mu\text{m}$ , and the total scan time was 640 s.  $T_2$  maps, which display the spatial distribution of the  $T_2$  values on colour-scale images, were generated from 32 sequential images with the image sequence analysis tool in the ParaVision image program. The  $T_2$  value in each voxel was calculated using Eq. 4:

$$M = M_0 \exp(-t / T_2) \quad (\text{Eq. 4})$$

where,  $M$ : signal intensity at echo time  $t$ , and  $M_0$ : signal intensity at echo time zero.

A total of five cross-sectioned  $T_2$  maps were obtained by a dry-cured ham model from each of the two drying conditions. One of the measurements was made on the sample before drying. Other measurements were made on the samples during and after drying under drying conditions of 70 and 10% RH at 18°C.

#### Energy consumption

The current consumption of the drying chamber in each drying condition was recorded at 5-min intervals with a clamp wattmeter (LR5051, HIOKI Corp., Japan). Then, the total energy consumption was calculated by integrating the time up to a moisture content 175% d.b. of the samples. The total average energy consumption and the average specific energy consumption were also calculated.

## Results and discussion

### Drying time and moisture content

Changes in the drying rate over time during the drying experiments at RH values of 10, 40, and 70% at temperatures of 18, 27, and 35°C are shown in Figure 2.

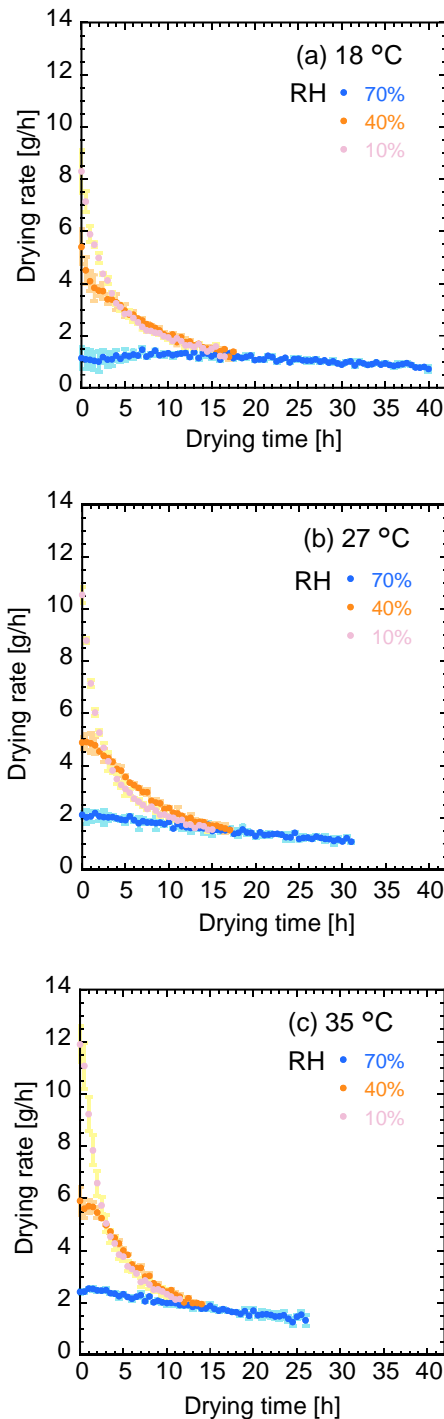


**Figure 2.** Relationships between the drying rate and time at 18°C (a), 27°C (b), and 35°C (c) under RH values of 10, 40, and 70%. Standard errors are shown with light colours.

At any temperature condition, the lower the RH, the faster the drying rate. Under the conditions of low RH of 10 and 40%, the drying rate at the initial stage of drying was remarkably high, and the drying rate decreased as drying time progressed. However, under the condition of RH of 70%, the drying rate decreased steadily from the initial stage to the late stage of drying, and no rapid change in the drying rate was observed.

Changes in the moisture ratio ( $W_R$ ) over time during the drying experiments at RH values of 10, 40, and 70% at temperatures of 18, 27, and 35°C are shown in Figure 3. Drying of all the samples was the falling-rate period because the slope of the tangent line became smaller with increasing drying time. From the relationship between  $W_R$  and drying time, a faster decrease in  $W_R$  was observed at a higher temperature at the same RH value.

From Eq. 2, the values of  $D_e$  under different humidity conditions were calculated for each temperature. Changes in the  $D_e$  values with the moisture content as the drying progressed, under the three different humidity conditions, are shown in Figure 4. The changes in the  $D_e$  values were different depending on the RH conditions during the drying. The  $D_e$  values were higher at a lower RH value for the same moisture content. The same analysis has also been applied to Japanese noodles (Inazu *et al.*, 2002) and yams (Ju *et al.*, 2016). Similar to the results reported in the present work, the  $D_e$  values were higher when the RH was low.

In Gou *et al.* (2004), the  $D_e$  values for dry-cured ham ranged from  $0.239 \times 10^{-10}$  to  $0.779 \times 10^{-10}$  m<sup>2</sup>/s (19°C). When comparing these values with the  $D_e$  values ranging from  $2.10 \times 10^{-10}$  to  $13.9 \times 10^{-10}$  m<sup>2</sup>/s (18°C) shown in Figure 4a and Table 1, it was found that the values in the Japanese dry-cured ham model were approximately 10× to 20× larger. This difference could have been due to the different meat used in the samples for drying; minced versus chunk. In chunk meat, the moisture transfers from the inside of the muscle fibres to the surface, and then evaporates. In contrast, the samples in the present work were prepared using minced meat where the free water in the brine could easily transfer through the gap between the meat grains.

Regarding Figure 4, the  $D_e$  values at 10% RH drastically decreased as the moisture content decreased in the initial stage of drying, whereas the  $D_e$  values at 40% RH gradually decreased, and the  $D_e$  values at 70% RH were almost

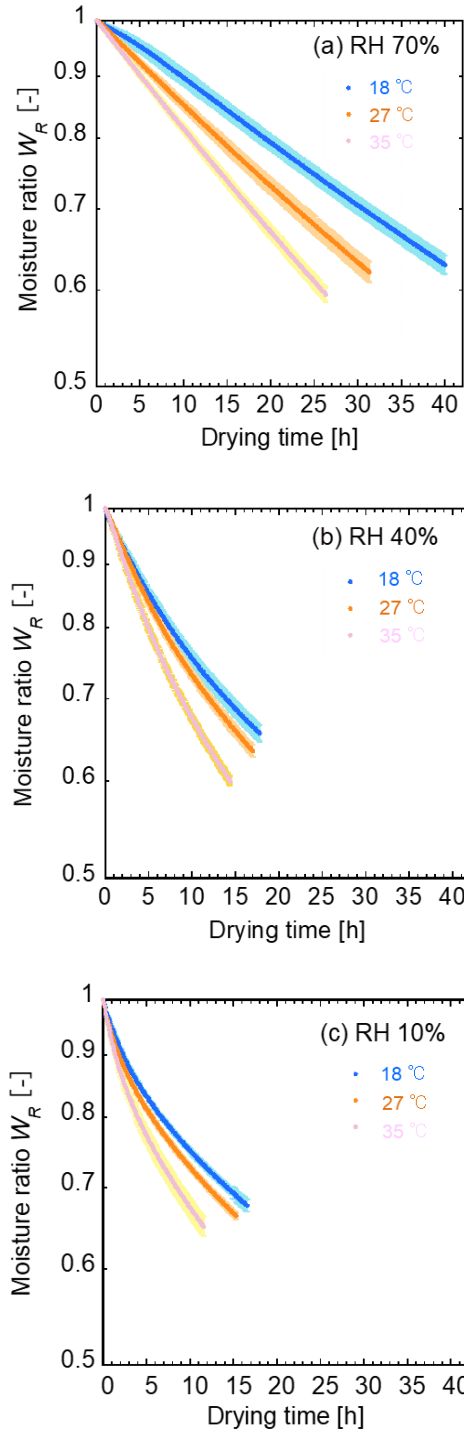


**Figure 3.** Relationships between the moisture ratio and drying time at RH values of 70% (a), 40% (b), and 10% (c) at temperatures of 18, 27, and 35°C. Mean values ( $n = 3$ ) are plotted with dark colours, whereas the standard errors are shown with light colours.

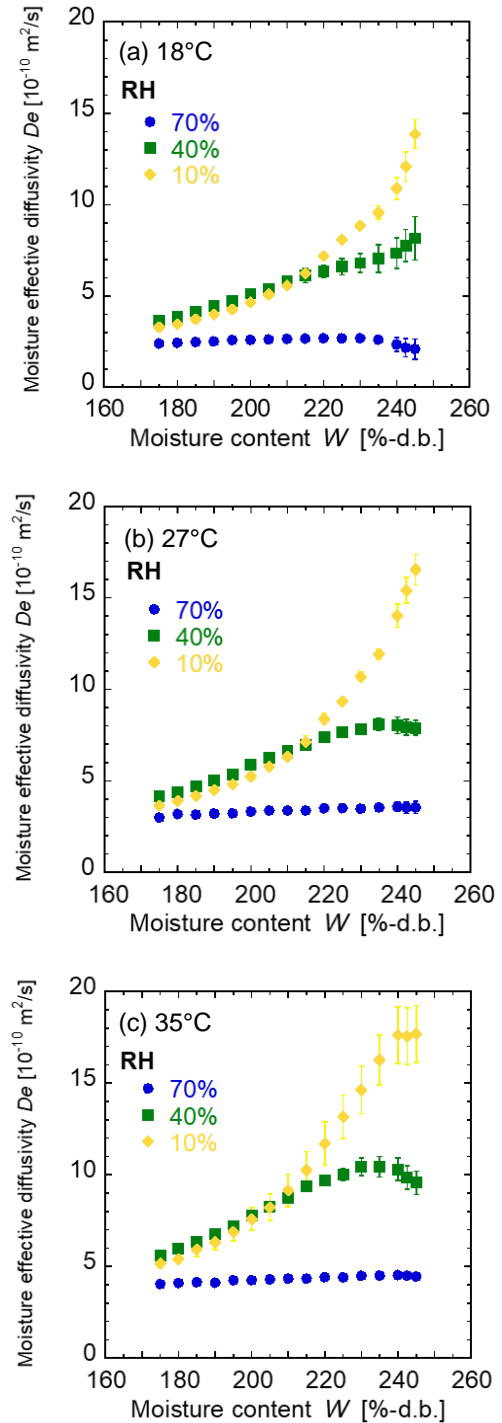


**Figure 4.** Changes in the moisture effective diffusivity ( $D_e$ ) values with changing moisture content ( $W$ ) at different RH conditions at 18, 27, and 35°C. Standard errors are shown with bars for each plot.

constant during drying. These differences suggested that there was a difference in the moisture transfer in the drying samples depending on RH conditions.

#### Activation energy

The values of the activation energy  $E_a$  calculated from Eq. 3 are shown in Figure 5 as a function of the moisture content. The activation energy changed with the moisture content in accordance with the progression of the drying. When the RH was low at 10%, the activation energy drastically increased with decreasing moisture content until  $W = 235\%$  d.b., then decreased to an almost constant value. In contrast, under 40 and 70% RH conditions, the activation energy gradually increased with decreasing moisture content, then was almost constant. In the late stage of drying (*i.e.*, below  $W = 185\%$  d.b.), the activation energies had similar values of approximately 19 kJ/mol even under different RH conditions.

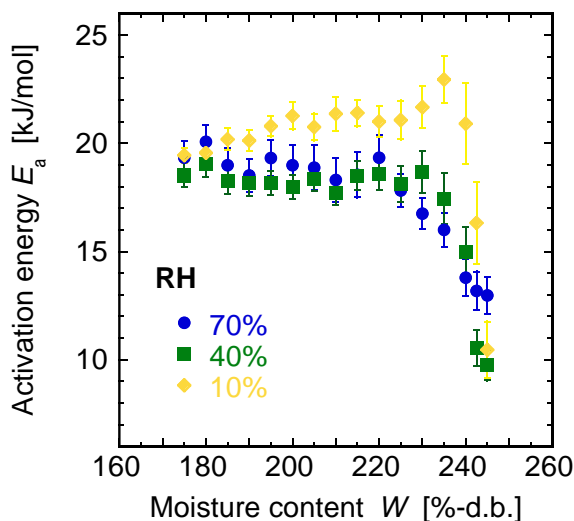


**Figure 5.** Changes in the activation energy ( $E_a$ ) values with the moisture content ( $W$ ) under different RH conditions. Standard errors are shown with bars for each plot.

In the initial stage of drying ( $W$ : from 245 to 235% d.b., approximately), the increase in the activation energy at low 10% RH corresponded to the fast transfer of moisture from the surface. Higher  $D_e$  values in the initial drying stage at 10% RH (Figure 4) imply fast transfer of moisture from the surface. The surface of the sample was dried and hardened temporarily by the fast transfer and evaporation of moisture from the surface. This fast transfer corresponded to an increase in the potential energy barrier for the diffusion of moisture, and thus, the

activation energy was drastically increased in the initial stage of drying under low RH conditions. During drying of dry-cured ham, it has been reported that RH has a substantial effect on the drying rate (Petrova *et al.*, 2015). In particular, low RH and high temperatures cause case hardening; *i.e.*, formation of dried and hard regions on the surface of the drying samples. Case hardening leads to restricted moisture transfer in the drying sample. It is probable that such case hardening occurred during the drying in the Japanese dry-cured ham model.

In the middle to late stages of drying ( $W$ : from 235 to 175% d.b., approximately) under low 10% RH condition, the dryness of the partly dried surface was alleviated by the transfer of moisture from the inside of the sample; consequently, the activation energy gradually decreased, and was almost constant in the late drying stage, to the similar values as at 40 and 70% RH ( $W < 190\%$  d.b.).

In a previous study, a high-humidity treatment that temporarily increased the humidity during drying (poultice up process; PUP) was reported (Konishi and Kobayashi, 1999; Konishi *et al.*, 2001a; 2001b). By this PUP, the moisture in the environment migrated to the surface of the drying sample, and then the partly dried surface was wetted. This wetting reduced the potential energy barrier of the moisture diffusion, and thus the activation energy decreased. Consequently, moisture transfer from the inside to the surface was promoted, thus resulting in a reduction in the total drying time (Konishi and Kobayashi, 2003).

In our experiments, in the middle to late stages of drying ( $W$ : from 235 to 175% d.b., approximately) at low 10% RH, moisture was supplied from the inside to the surface of the samples, similar to the PUP (although the moisture was not from the outside but from the inside); therefore, the activation energy gradually decreased.

Activation energy of  $D_e$  at 40 and 70% RH conditions increased with decreasing moisture content throughout drying. Under these humid conditions, case hardening would not occur; therefore, the activation energy did not drastically change when compared with that of low 10% RH in the initial stage of drying.

#### Moisture distribution by MRI analysis

The moisture distribution inside the dry-cured ham model during drying was evaluated by MRI. Figure 6 shows a map of the  $T_2$  relaxation time by MRI before drying (Figure 6a), during drying (Figure

6b-1 and 6c-1), and after drying (Figure 6b-2 and 6c-2) samples under an RH of 70 and 10% at 18°C. The  $T_2$  relaxation time reflects the moisture of the sample; the longer the  $T_2$ , the higher the moisture (Sekiyama et al., 2012). The dry-cured ham model, in which the moisture content was measured in advance, was evaluated by MRI. The  $T_2$  value was obtained, and a calibration curve for moisture content was calculated from the  $T_2$  value. Based on the calibration curve, Figure 7 indicates the relationship between the distance from the surface of the sample and the moisture content from the  $T_2$  relaxation time of the

dry-cured ham model when the drying condition was 70% RH (Figure 7a) and 10% RH (Figure 7b) at 18°C. The moisture content of the entire dry-cured ham model is indicated in Figure 7.

From Figure 6a, the  $T_2$  values of the dry-cured ham model before drying were almost uniformly distributed on the surface and centre of the sample. From Figures 6b and 6c, during the middle to late stages of drying, the  $T_2$  value decreased from the surface with increasing time regardless of the drying conditions. However, under the drying condition of 10% RH (Figure 6c-1), the  $T_2$  value in the near-

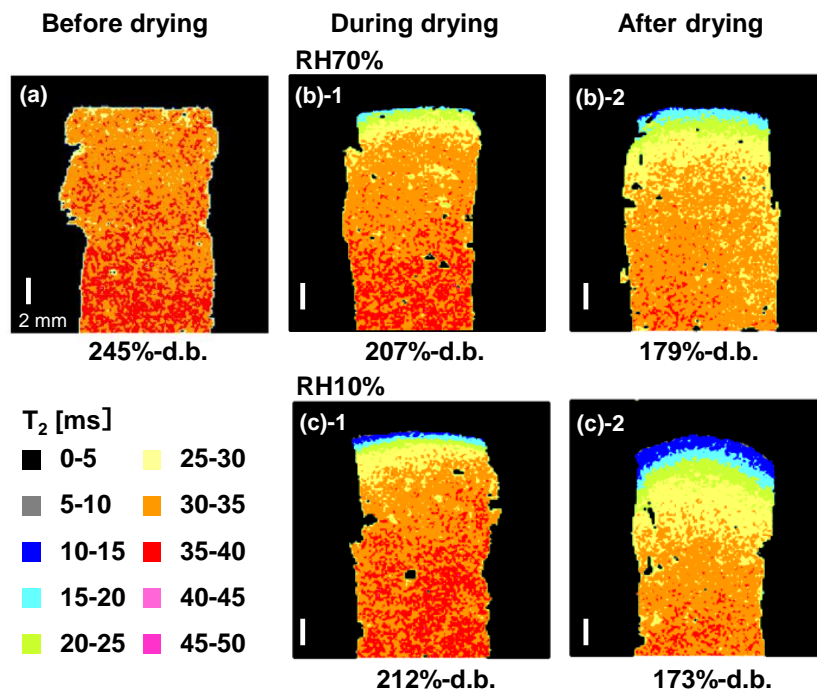


**Figure 6.** Maps of spin-spin relaxation time ( $T_2$ ) of the cross section of the Japanese dry-cured ham model at 18°C before drying (a), during drying under RH values of 70% (b-1) and 10% (c-1), and after drying under RH values of 70% (b-2) and 10% (c-2).

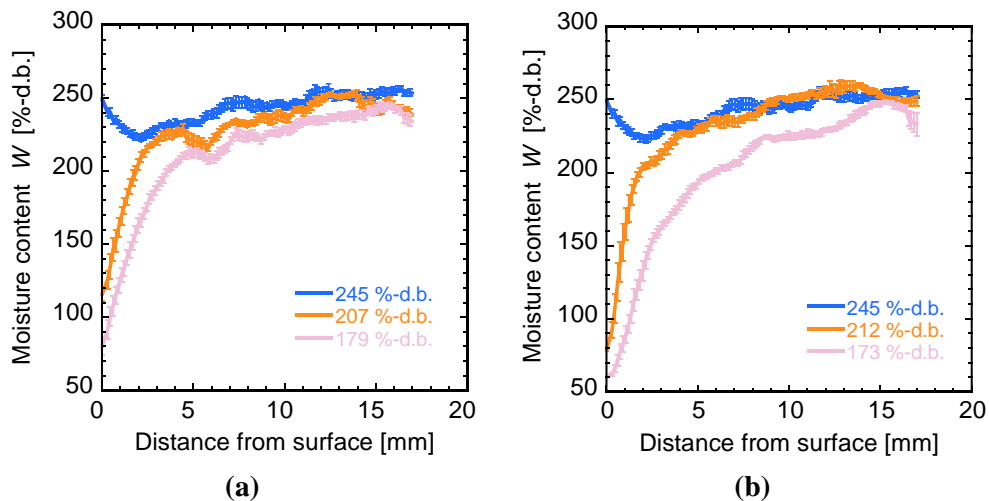


**Figure 7.** Internal moisture contents ( $W$ ) of the dry-cured ham model during drying conditions under RH values of 70% (a) and 10% (b) at 18°C.

surface region was significantly lower than that of 70% RH (Figure 6b-1). In particular, in Figure 6c-1,  $T_2$  near the surface had a value of 10 - 15 ms, thus indicating the very low moisture content. Moreover, in accordance with the moisture content distribution at 212% d.b. in Figure 7b, the moisture content decreased drastically near the surface (up to approximately 2 mm from the surface). From these results by MRI, case hardening of the surface occurred at 10% RH as discussed earlier.

In the late stage of drying (173% d.b.) at 10% RH (Figure 7b), the moisture distribution near the surface (up to approximately 2 mm from the surface) no longer exhibited a sharp difference in the moisture

concentration when compared with that of the initial to the middle stages of drying (212% d.b.). This change of moisture distribution suggested that moisture was supplied from the inside to the surface of the samples, similar to the PUP (although the moisture was not from the outside but from the inside) as discussed earlier.

#### Energy consumption

In the context of practical applications, the energy consumption of the drying chamber was measured. The drying time and energy consumption, up to the specified moisture content (*i.e.*, 175 % d.b.) under each condition are shown in Table 2.

**Table 2.** Energy consumption and drying time of Japanese dry-cured ham model under different drying conditions.

Drying condition		Drying time (h)*	Energy consumption (MJ)	Total average energy consumption (MJ/kg sample)	Average specific energy consumption (MJ/kg water removed)	Desiccant dehumidifier
(%)	(°C)					
10	18	16.6	128.9	195.3	888.8	ON
	27	15.3	118.1	178.9	814.3	ON
	35	11.6	93.2	141.3	643.0	ON
40	18	17.8	142.9	216.5	986.7	ON
	27	17.0	127.1	192.5	876.4	ON
	35	14.4	66.6	100.9	459.3	OFF
70	18	40.0	169.9	257.5	1171.9	OFF
	27	31.3	144.4	218.7	995.6	OFF
	35	26.3	126.0	190.9	869.0	OFF

\* The drying time up to a moisture content of 175% d.b.

The drying time required to reach the specified moisture content was shorter as the drying temperature increased, and shorter as the drying humidity decreased. The energy consumption was calculated by summing the electric power consumed during the drying time. Under the conditions of 18 and 27°C, the energy consumption was lower at higher drying temperatures and lower RH because of the longer drying time.

However, at 35°C, the energy consumption was the lowest under the condition of 40% RH. This is because the desiccant dehumidifier equipped in the drying chamber did not operate under this drying condition. The humidity of this drying chamber was always controlled by the compressor, but the desiccant dehumidifier was additionally turned on under low-temperature and low-humidity conditions. This desiccant dehumidifier consumed a large

quantity of electric power. Therefore, under the condition that the desiccant dehumidifier operates, the energy consumption was high, as shown in Table 2.

In the context of energy consumption, the drying condition of 35°C and 40% RH was the most efficient. However, optimal conditions must be chosen with regard to the energy consumption and the quality of the Japanese dry-cured ham.

The total average energy consumption and average specific energy consumption were 100.9 - 257.5 MJ/kg sample and 459.3 - 1171.9 MJ/kg water removed, respectively, as shown in Table 2. These values were higher than the values reported in the drying of freshwater fishes (Khan *et al.*, 2020), despite that the samples were dried from about 245 to 175% d.b. in the present work, while from about 275 to 45% d.b. in the previous report. With respect to the

weights of the sample per drying chamber, the value was 1.6 kg sample/m<sup>3</sup> in the present work, while it was approximately 7.9 kg sample/m<sup>3</sup> in the previous report (Khan *et al.*, 2020). A larger sample weight per drying chamber would allow the efficient use of thermal energy from the blowing air for drying, therefore there was a difference in the total average energy consumption. In the present work, only three samples were placed in the drying chamber for analysing the drying behaviour of Japanese dry-cured ham. The total average energy consumption could be improved if more samples were placed in the drying chamber.

## Conclusion

Using a Japanese dry-cured ham model containing uniformly distributed brine, the  $D_e$  values under different drying conditions were determined. The moisture transfer during drying was discussed in the context of the changes in the activation energy and the moisture distribution determined by MRI analysis. Furthermore, the energy consumption in the different drying conditions was evaluated to investigate the energy efficiency.

Higher  $D_e$  values were obtained at lower 10% RH condition for the same moisture content of the drying ham. The activation energy of  $D_e$  at low 10% RH drastically first increased with decreasing moisture content in the initial stage of drying, then decreased to an almost constant value. In the initial stage of drying under this low RH, the drying rate was high. From the MRI analysis, the moisture content of the surface drastically decreased. Therefore, the surface of the Japanese dry-cured ham was dried and hardened temporarily (*i.e.*, case hardening) by the fast transfer of moisture from the surface. In the middle to late stages of drying, the activation energy gradually decreased to the similar values as at 40 and 70% RH in the late stage of drying. From the MRI analysis after drying, the moisture distribution near the surface no longer exhibited a sharp difference in moisture concentration. The partly dried state of the surface was alleviated by the transfer of moisture from the inside of the sample.

In contrast, the activation energy of  $D_e$  under 40 and 70% RH conditions increased with decreasing moisture content, and had an almost constant value in the late stage of drying. These suggested that the moisture diffused gradually from the inside to the surface of the sample without case hardening.

The drying time and energy consumption, up to the specified moisture content (*i.e.*, 175% d.b.), under each condition were measured. Under the condition that the desiccant dehumidifier operated, the energy consumption was high. In the context of energy consumption, the drying condition of 35°C and 40% RH was the most efficient. However, optimal condition must be chosen with regard to the power consumption and the quality of the Japanese dry-cured ham.

These findings revealed that the moisture transfer in the Japanese dry-cured ham model was greatly affected by the RH and temperature conditions. The obtained information and knowledge can facilitate the development of more-efficient drying processes for producing Japanese dry-cured ham.

## Acknowledgement

The authors thank Dr. Yasuyo Sekiyama (National Food Research Institute, NARO, Japan) for technical support in MRI experiments and analyses.

## References

- Carslaw, H. S. and Jaeger, J. C. 1959. Conduction of heat in solids. 2<sup>nd</sup> ed. New Jersey: Oxford University Press.
- Elmas, F., Bodruk, A., Köprüalan, Ö., Arikaya, S., Koca, N., Serdaroğlu, M. F., ... and Koç, M. 2020. Drying kinetics behavior of turkey breast meat in different drying methods. *Journal of Food Process Engineering* 43: e13487.
- Gou, P., Comaposada, J. and Arnau, J. 2002. Meat pH and meat fibre direction effects on moisture diffusivity in salted ham muscles dried at 5°C. *Meat Science* 61: 25-31.
- Gou, P., Comaposada, J. and Arnau, J. 2003. NaCl content and temperature effects on moisture diffusivity in the *Gluteus medius* muscle of pork ham. *Meat Science* 63: 29-34.
- Gou, P., Comaposada, J. and Arnau, J. 2004. Moisture diffusivity in the lean tissue of dry-cured ham at different process times. *Meat Science* 67: 203-209.
- Hallström, B. 1990. Mass transport of water in foods - A consideration of the engineering aspects. *Journal of Food Engineering* 12(1): 45-52.
- Inazu, T., Iwasaki, K. and Turuta, T. 2002. Effect of temperature and relative humidity on drying

- kinetics of fresh Japanese noodle (udon). *LWT – Food Science and Technology* 35: 649-655.
- Ismail, O. 2017. An experimental and modeling investigation on drying of chicken meat in convective dryer. *Studia Universitatis Babeş-Bolyai Chemia* 62(4): 459-469.
- Ju, H.-Y., El-Mashad, M. H., Fang, X.-M., Pan, Z., Xiao, H.-W., Liu, Y.-H. and Gao, Z.-J. 2016. Drying characteristics and modeling of yam slices under different relative humidity conditions. *Drying Technology* 34(3): 296-306.
- Khan, M. A., Moradipour, M., Obeidullah, M. and Quader, A. K. M. A. 2020. Heat and mass transport analysis of the drying of freshwater fishes by a forced convective air-dryer. *Journal of Food Process Engineering* 44(3): e13574.
- Konishi, Y. and Kobayashi, M. 1999. Dynamic characterization of moisture diffusion behavior in a fish paste sausage during poultice up process operated in the course of forced ventilation drying. *Nippon Shokuhin Kagaku Kogaku Kaishi* 46(4): 205-211.
- Konishi, Y. and Kobayashi, M. 2003. Characteristic innovation of a food drying process revealed by the physicochemical analysis of dehydration dynamics. *Journal of Food Engineering* 59: 277-283.
- Konishi, Y., Horiuchi, J. and Kobayashi, M. 2001a. Dynamic evaluation of the dehydration response curves of foods characterized by a poultice-up process using a fish-paste sausage. I. Determination of the mechanism for moisture transfer. *Drying Technology* 19(7): 1253-1270.
- Konishi, Y., Horiuchi, J. and Kobayashi, M. 2001b. Dynamic evaluation of the dehydration response curves of foods characterized by a poultice-up process using a fish-paste sausage. II. A new tank model for a computer simulation. *Drying Technology* 19(7): 1271-1285.
- Mewa, E. A., Okoth, M. W., Kunyanga, C. N. and Rugiri, M. N. 2018. Drying modelling, moisture diffusivity and sensory quality of thin layer dried beef. *Current Research Nutrition and Food Science* 6(2): 552-565.
- Okos, M. R., Narsimhan, G., Singh, R. K. and Weitnauer, A. C. 1992. Food dehydration. In Heldman, D. R. and Lund, D. B. (eds). *Handbook of Food Engineering*. New York: Marcel Dekker.
- Panagiotou, N. M., Krokida, M. K., Maroulis, Z. B. and Saravacos, G. D. 2004. Moisture diffusivity: Literature data compilation for foodstuffs. *International Journal of Food Properties* 7: 273-299.
- Petrova, I., Bantle, M. and Eikevik, T. M. 2015. Manufacture of dry cured ham: A review. Part 2. Drying kinetics, modeling and equipment. *European Food Research Technology* 241: 447-458.
- Sekiyama, Y., Horigane, A. K., Ono, H., Irie, K., Maeda, K. and Yoshida, M. 2012.  $T_2$  distribution of boiled dry spaghetti measured by MRI and its internal structure observed by fluorescence microscopy. *Food Research International* 48(2): 374-379.
- Tanaka, Y., Tsuzuku, T., Takahashi, T. and Suzuki, A. 2000. U.S. patent no. 6,014,926A - Injection into meat and pickle injector for use therein. United States: US Patent.